A Case Study of an Anomalous Cold-season Easterly Jet Streak in the Mid-latitudes

SCOTT M. ROCHETTE
Department of the Earth Sciences, The College at Brockport, State University of New York, Brockport, NY

PATRICK S. MARKET
Department of Soil, Environmental and Atmospheric Sciences, University of Missouri–Columbia, Columbia, MO

(Manuscript received 21 December 2010; in final form 30 July 2011)

ABSTRACT

A brief case study is provided of a rare, easterly upper-tropospheric jet streak that occurred in the mid-latitudes during a recent cold season. This event is significant because of the magnitude of the parent storm, which was the third major East Coast snowstorm in February 2010, delivering in excess of 50 cm (20 in.) of snow to large areas of New York and Vermont. The magnitude of the 300-hPa jet maximized some 18 hours after the related surface cyclone reached its minimum sea level pressure (972 hPa).

The relative uniqueness of this jet streak is established. Diagnostic analyses showed striking similarities between this well-defined easterly jet and the classic "four-quadrant" model for an upper-tropospheric, westerly linear jet streak, although many of the features are simply reversed in their expected positions (e.g., the jet's entrance region is found to the east of the jet core). The entrance region was particularly well-defined, with the ageostrophic wind directed southward toward lower heights, and divergence in the right entrance (northeast) region. The exit region exhibited a vertical motion field that was displaced southward of its expected location, but nevertheless showed a distinct divergent left exit region and ageostrophic flow toward higher heights north of the jet axis. Analysis of $\mathbf{Q_n}$ revealed the presence of a well-defined direct thermal circulation (DTC) in the jet's entrance region, with a weaker signal in the exit region. Cross-sectional analyses corroborated the better definition of the entrance region.

1. Introduction

The influence of upper-tropospheric jet streaks on sensible mid-latitude weather is well-known and well-documented (e.g., Beebe and Bates 1955; Uccellini and Johnson 1979; Uccellini and Kocin 1987; Rose et al. 2004; Clark et al. 2009). Most operational meteorologists are

Corresponding author address: Dr. Scott M. Rochette, Department of the Earth Sciences, The College at Brockport, State University of New York, 350 New Campus Drive, Brockport, NY 14420
E-mail: rochette@esc.brockport.edu

undoubtedly familiar with the four-quadrant model of the idealized jet streak (Fig. 1), but finding real-life examples that fit the conceptual model is more of a challenge, resulting from the influence of curvature (Beebe and Bates 1955; Moore and VanKnowe 1992) and/or thermal advection (Shapiro 1983). Finding such an ideal jet streak with *easterly* winds is even more difficult. The authors discovered such a well-defined easterly jet streak in late February 2010, in conjunction with a significant New England extratropical cyclone. The anomalous jet streak is the focus of this study, which is diagnosed via basic and derived kinematic fields. The data and methodology of this brief case study are outlined in section two. Section three offers the synoptic setup and morphology of the jet streak in question, establishes the relative rarity of easterly jet streaks in the cold-season mid-latitude atmosphere, and illustrates the jet streak at its relative peak through basic plan-view and cross-sectional analyses, as well as its influence on sensible weather. The case study is drawn to a close in section four, which offers perspective into the ramifications of the jet streak.

2. Data and method

Unless otherwise noted, the data used in this study to analyze the jet streak morphology are 0-h forecasts from the North American Mesoscale (NAM) model (Janjić et al. 2001) for the period from 1200 UTC 26 February to 0000 UTC 1 March 2010. These model output fields are displayed on the 81-km NAM 211 grid, as well as appropriate cross-sections. Observed upper-air data were used to help establish the unusual nature of this jet streak. At the time of the event (late February 2010), several of the radiosonde flights from Albany, NY, were unavailable. In

their stead, winds were estimated from the initial fields of the Rapid Update Cycle (RUC; Benjamin et al. 2004).

3. Analysis

a. Synoptic-scale features

A late-winter cyclone began to take shape east of Florida at 0000 UTC 25 February 2010, intensifying 26 hPa in 24 h as it moved southeast of Cape Cod, reaching a minimum pressure of 972 hPa. The cyclone became vertically stacked by 1200 UTC 26 February, when it retrograded toward New York City. Over the next 60 h the surface low-pressure system would continue to fill and drift over New York State, eventually dissipating by 0000 UTC 1 March 2010. Snowfall amounts in excess of 50 cm (20 in.) were reported for portions of New York and Vermont. An excerpt from the 1200 UTC 26 February 2010 area forecast discussion (AFD) from the Buffalo National Weather Service Forecast Office (NWSFO BUF) is included below:

> SYSTEM IS COMPLETELY BIZARRE AND ORIENTED A GOOD 90 DEGREES OFF A "NORMAL" COASTAL STORM WITH WARM AIR SURGING WESTWARD TO THE STORM`S NORTH ON HEELS OF A 65 KT 850 MB EASTERLY JET...WHILE COLD AIR GETS DRAWN INTO THE SOUTHERN AND EVEN SOUTHEAST FLANK OF THE STORM WITH SOME INCREDIBLE (12MB/3HR) PRESSURE RISES OVER CAPE COD...JUST A FEW HOURS AFTER SIMILAR FALLS IN THE SAME PLACE.

At 0000 UTC 26 February 2010 a closed 300-hPa low was centered over the Mid-Atlantic States, and an anomalous southeasterly jet took shape over New York and Pennsylvania. The closed low would continue to wobble over the northeastern U.S. over the next three days, resulting in a weak but distinct jet that rotated around the low in a counterclockwise fashion

(Figs. 2a-g), in addition to the larger and much stronger jet that remained on the low's equatorward side. The former jet's evolution is shown clearly in Fig. 2h.

The National Oceanic and Atmospheric Administration's (NOAA) Hydrometeorological Prediction Center (HPC) satellite/surface analysis composite valid at 0000 UTC 27 February 2010 (Fig. 3), the time at which the easterly jet was best defined, reveals a large cyclonic cloud shield over the northeastern U.S., with a pair of low-pressure centers located over eastern Long Island (992 hPa) and extreme southern Nova Scotia (994 hPa). A water vapor imagery perspective of the tightly wound system is provided in Fig. 4. Note that the easterly jet streak is detectable by the sharp gradient in the water vapor field, with the 'moist' air appearing on the anticyclonic side of the jet, in this case on the jet's northern side, opposite of convention. A national radar mosaic at this time (Fig. 5) showed organized precipitation over central New England extending westward into central and eastern New York, along with a separate area covering much of Maine and New Brunswick. Wrap-around precipitation occurred over most of the Great Lakes region, with some lake enhancement downwind of Lakes Superior, Michigan, Huron, and Erie.

b. Determination of event uniqueness

In order to establish the relative significance of this event, wind data for the 300-hPa level over Albany, NY, were obtained from the University of Wyoming online data portal (http://weather.uwyo.edu/upperair/sounding.html) for the months of February and March during the 10-year period of 1999-2008. Both the 0000 UTC and 1200 UTC flights were considered in this analysis. Out of the potential 1186 soundings, 109 were missing or had missing data; as

such there were 1077 soundings available for analysis. Only 38 (~3.5%) of the remaining sample had a 300-hPa wind that was from the east, with a mean (median) easterly wind component of -9.0 m s^{-1} (-7.4 m s^{-1}) and a distinct skew toward weaker (closer to zero) values.

During the period of interest, we also examined sounding data for Albany, NY from 0000 UTC 26 February 2010 to 1200 UTC 28 February 2010. Unfortunately, observed data were available for Albany, NY, only at 0000 UTC 26 February 2010 and 1200 UTC 28 February 2010. Estimates for the 300-hPa winds for Albany, NY, were derived from the 20-km RUC model initial fields at these intermediate times:

- 1200 UTC 26 February 2010
- 0000 UTC 27 February 2010
- 1200 UTC 27 February 2010
- 0000 UTC 28 February 2010

The strongest easterly wind component in this event was observed at 0000 UTC 26 February 2010 at -29.1 m s^{-1}. This value was exceeded only once before during the 1999-2008 period that we examined; that date was 1200 UTC 28 March 2004.

Results for this same analysis on 300-hPa data from Maniwaki, QC (CWMW) were very similar. Out of the potential 1186 soundings, 50 were missing or had missing data; as such there were 1136 soundings available for analysis. Only 75 (~6.6%) of the remaining sample had a 300-hPa wind that was from the east, with a mean (median) easterly wind component of -8.3 m s^{-1} (-6.2 m s^{-1}) and a distinct skew toward weaker (closer to zero) values. As with the Albany analysis, the maximum jet value of -29.1 m s^{-1} at 0000 UTC 26 February 2010 was exceeded only once before at CWMW during the 1999-2008 period that we examined; that date was 1200 UTC 23 March 2006.

To further illustrate the relatively rare nature of this jet streak, an analysis of standardized U-wind anomalies at 300 hPa (Fig. 6) was generated from the North American Regional Reanalysis (NARR; Mesinger et al. 2006) dataset, which revealed anomalies of 3 and 4 standard deviations. In addition, the NARR dataset was interrogated for analogous 300-hPa patterns to the event in question (e.g., Gravelle et al. 2009). Five episodes of 90-kt easterly 300-hPa jet streaks were found in the 30+ year dataset. Clearly, the event studied here was an outlier, and deserving of additional scrutiny.

c. Diagnosis of the easterly jet streak

Further examination of the easterly jet in question focuses on the 0000 UTC 27 February 2010 timeframe (Fig. 7), as the jet was best defined at this time, located over northern New England and southern Quebec. In order for an easterly jet streak to occur, there would need to be a reversal of the normal north-south temperature gradient, seen here in the 1000-500 hPa thickness field (Fig. 8). As a likely result of this thermal configuration (and the significant warm advection associated with a strong low-level jet—see below), rain is falling over the Canadian Maritimes (Fig. 9), while most of the precipitation associated with this system is snow.

Figure 10 illustrates the jet's structure and distribution of divergence at 0000 UTC 27 February 2010. The entrance and exit regions of the jet are located in an opposite sense as those found with a westerly jet streak (see example in Fig. 1), although they are properly located from a flow-relative sense, as air would have been entering the jet streak from the east. Nonetheless, significant divergence is revealed in the left exit region (southwest of the jet core) and right entrance region (northeast of the core). While not as distinct as the divergent areas, convergent

regions are, nevertheless, evident in the left entrance and right exit quadrants. Also noteworthy is the orientation of the jet-level ageostrophic wind field, shown in the wind barbs. The entrance region is very well-defined, with the ageostrophic wind directed toward lower heights, indicating the conversion of potential to kinetic energy as air parcels accelerate toward the jet core. The exit region is defined by an ageostrophic flow toward higher heights (thereby converting kinetic energy to potential energy), with a corresponding deceleration as air parcels leave the jet core.

In order to properly diagnose the jet streak's divergent and convergent regions, analyses of Q-vector divergence were parsed into components along and normal to the thermal gradient ($\mathbf{Q_s}$ and $\mathbf{Q_n}$, respectively; see Keyser et al. 1988, 1992; Barnes and Colman 1993; and Billingsley 1998). Convergence and divergence of $\mathbf{Q_s}$ would generally depict the ascent/descent pattern commonly associated with synoptic-scale upper-level troughs, while convergence and divergence of $\mathbf{Q_n}$ would highlight the effects of the thermally direct and indirect circulations in the jet streak's entrance and exit regions, respectively. Examination of the 400-700 hPa $\nabla\cdot \mathbf{Q_s}$ analysis (Fig. 11) shows strong areas of $\mathbf{Q_s}$ divergence and convergence primarily on the equatorward (cyclonic shear) side of the jet, with two weak upward vertical motion (UVM) maxima bookending an area of sinking motion (each at 500 hPa) over eastern Pennsylvania and New Jersey. These weak regions of vertical motion are linked to the mid-tropospheric trough and areas of associated absolute vorticity advection (not shown). The analysis of 400-700 hPa $\nabla\cdot \mathbf{Q_n}$ (Fig. 12) and 500-hPa omega reveals generally weaker regions of $\mathbf{Q_n}$ convergence (cf. Fig. 11); nevertheless, a very distinct signal of a direct thermal circulation (DTC) exists in the jet's entrance region, with strong rising motion collocated with a well-defined area of $\mathbf{Q_n}$ convergence. An area of strong downward vertical motion (DVM) appears in the jet's left entrance region, which was linked to an area of distinct $\mathbf{Q_n}$ divergence. The jet's exit region

signal is not as strong as that found in the entrance region, and the $\mathbf{Q_n}$ divergence/convergence couplet (and associated DVM/UVM) appear displaced to the south of the jet axis. It should be noted that the fields of explicit vertical motion included in Figs. 11 and 12 (as well as subsequent figures) express *model* vertical motion, while the $\nabla\cdot \mathbf{Q_s}$ and $\nabla\cdot \mathbf{Q_n}$ fields imply *quasigeostrophic* vertical motions only. Nevertheless, these divergence/convergence fields do indicate a clear quasigeostrophic (and familiar) contribution to vertical motion from the jet streak.

To further examine the structure and associated circulations with this jet streak, cross-sections through the jet's entrance and exit regions were constructed. The cross-section axes (orientations shown in Fig. 10) were chosen using two criteria: the location of the divergence-convergence couplet, and the orientation of the jet-level ageostrophic wind (toward lower [higher] heights in the jet's entrance [exit] region). A cross-section (Fig. 13) through the jet's entrance region at 0000 UTC 27 February 2010 runs from Havre-Saint-Pierre, QC (CYGV, north) to a point in the Atlantic Ocean 170 km east of Nantucket Island, MA (41˚N, 68˚W, south). A well-defined DTC is evident, with significant rising motion ($\omega \leq -14$ μb s^{-1}) underneath the right entrance (north) side of the jet. The sinking portion of the DTC is somewhat weaker ($\omega \geq 6$ μb s^{-1}), but still evident. A significant easterly low-level jet (LLJ) is apparent in the lower troposphere (~850 hPa), under the right entrance region of the upper-level jet streak. Note the sloping zone of upward vertical motion (UVM) south of the LLJ (Uccellini and Johnson 1979; COMET 2010). Figure 14 illustrates the aforementioned LLJ in plan view. By contrast, the cross-section through the exit region (Fig. 15), which runs from Moosonee, ON (CYMO, north) to Elkins, WV (EKN, south), is not as well-defined as the entrance region cross-section, but still significant. Based on the conceptual model, one would expect to see rising motion on the south side of the jet, which is present but weaker ($\omega \leq -6$ μb s^{-1}) than that found

under the right entrance region. Sinking motion is very weak and found directly under the jet, instead of under the right exit region as predicted by the conceptual model.

4. Conclusions

This study focused on the development and diagnosis of an upper-tropospheric jet streak that is unique from two perspectives: it was a rare easterly jet in the mid-latitudes (cf. tropical easterly jet stream; Koteswaram 1958), and it conformed quite well to the established four-quadrant conceptual model, with the exception that the entrance and exit regions were reversed (to the east and west of the jet core, respectively) with respect to the well-known model of a westerly jet streak. However, the divergent and convergent regions of the jet streak were generally well-placed (in a flow-relative sense) with respect to the conceptual model, found to the northeast/southwest and northwest/southeast of the jet core, respectively. The jet streak influenced sensible weather (through UVM) under its divergent regions, which was corroborated via diagnosis of $\mathbf{Q_n}/\mathbf{Q_s}$ vectors. The DTC and vertical motion fields associated with the jet's entrance region were nearly textbook examples, while the exit region vertical motion field was similarly well-defined but displaced southward of the expected location with respect to the conceptual model.

Acknowledgements. The authors are indebted to Mr. Thomas McDermott of The College at Brockport for his expert assistance in data collection and interrogation for this case. Mr. Chad Gravelle (Saint Louis University) and Dr. Gustavo Pereira (The College at Brockport) offered

early reviews of the manuscript. Mr. Gravelle also provided Figures 6 and 9. Mr. Adam Hirsch (University of Missouri-Columbia) provided much-needed assistance in assembling the climatology used in this study. Dr. Steve Chiswell (Savannah River National Laboratory) supplied valuable guidance regarding Q-vector formulation in GEMPAK. Finally, the authors are especially grateful to Dr. Marty Baxter (Central Michigan University) and two anonymous reviewers for their valuable feedback that led to a stronger study.

REFERENCES

Barnes, S. L., and B. R. Colman, 1993: Quasigeostrophic diagnosis of cyclogenesis associated with a cutoff extratropical cyclone – the Christmas 1987 storm. *Mon. Wea. Rev.*, **121,** 1613-1634.

Beebe, R. G., and F. C. Bates, 1955: A mechanism for assisting in the release of convective instability. *Mon. Wea. Rev.*, **83,** 1-10.

Benjamin, S. G., and Coauthors, 2004: An hourly assimilation-forecast cycle: The RUC. *Mon. Wea. Rev.*, **132,** 495-518.

Billingsley, D. B., 1998: Review of QG theory – part III: A different approach. *Natl. Wea. Dig.,* **22:3,** 3-10.

Clark. A. J., C. J. Schaffer, W. A. Gallus, Jr., and K. Johnson-O'Mara, 2009: Climatology of storm reports relative to upper-level jet streaks. *Wea. Forecasting*, **24,** 1032-1051.

Cooperative Program for Operational Meteorology, Education and Training, cited 2011: Jet streak circulations. [Available online at http://www.meted.ucar.edu/norlat/jetstreaks/.]

Gravelle, C. M., C. E. Graves, J. P. Gagan, F. H. Glass, and M. S. Evans, 2009: Winter weather guidance from regional historical analogs. Preprints, *23rd Conf. on Weather Analysis and Forecasting*, Omaha, NE, Amer. Meteor. Soc., JP3.10. [Available online at http://ams.confex.com/ams/pdfpapers/154201.pdf.]

Janjić, Z. I., J. P. Gerrity, and S. Nickovic, 2001: An alternative approach to nonhydrostatic modeling. *Mon. Wea. Rev.*, **129,** 1164–1178.

Keyser, D., M. J. Reeder, and R. J. Reed, 1988: A generalization of Petterssen's frontogenesis function and its relation to the forcing of vertical motion. *Mon. Wea. Rev.*, **116,** 762-780.

_____, B. D. Schmidt, and D. G. Duffy, 1992: Quasigeostrophic diagnosis of three-dimensional ageostrophic circulations in an idealized baroclinic disturbance. *Mon. Wea. Rev.*, **120,** 698-730.

Koteswaram, P., 1958: The easterly jet stream in the Tropics. *Tellus*, **10,** 43–57.

Mesinger, F., and Coauthors, 2006: North American Regional Reanalysis. *Bull. Amer. Meteor. Soc.,* **87,** 343-360.

Moore, J. T., and G. E. VanKnowe, 1992: The effect of jet-streak curvature on kinematic fields. *Mon. Wea. Rev.,* **120,** 2429-2441.

Rose, S. F., P. V. Hobbs, J. D. Locatelli, and M. T. Stoelinga, 2004: A 10-yr climatology of relating the location of reported tornadoes to the quadrants of upper-level jet streaks. *Wea. Forecasting*, **19,** 301-309.

Shapiro, M. A., 1983: Mesoscale weather systems of the central United States. *The National STORM Program: Scientific and Technological Bases and Major Objectives.* R. A. Anthes, Ed., University Corporation For Atmospheric Research, P. O. Box 3000, Boulder, CO 80307, 3.1-3.77.

Uccellini, L. W., and D. R. Johnson, 1979: The coupling of upper and lower tropospheric jet streaks and implications for the development of severe convective storms. *Mon. Wea. Rev.*, **107,** 682-703.

_____, and P. J. Kocin, 1987: The interaction of jet streak circulations during heavy snow events along the East Coast of the United States. *Wea. Forecasting*, **2,** 289-308.

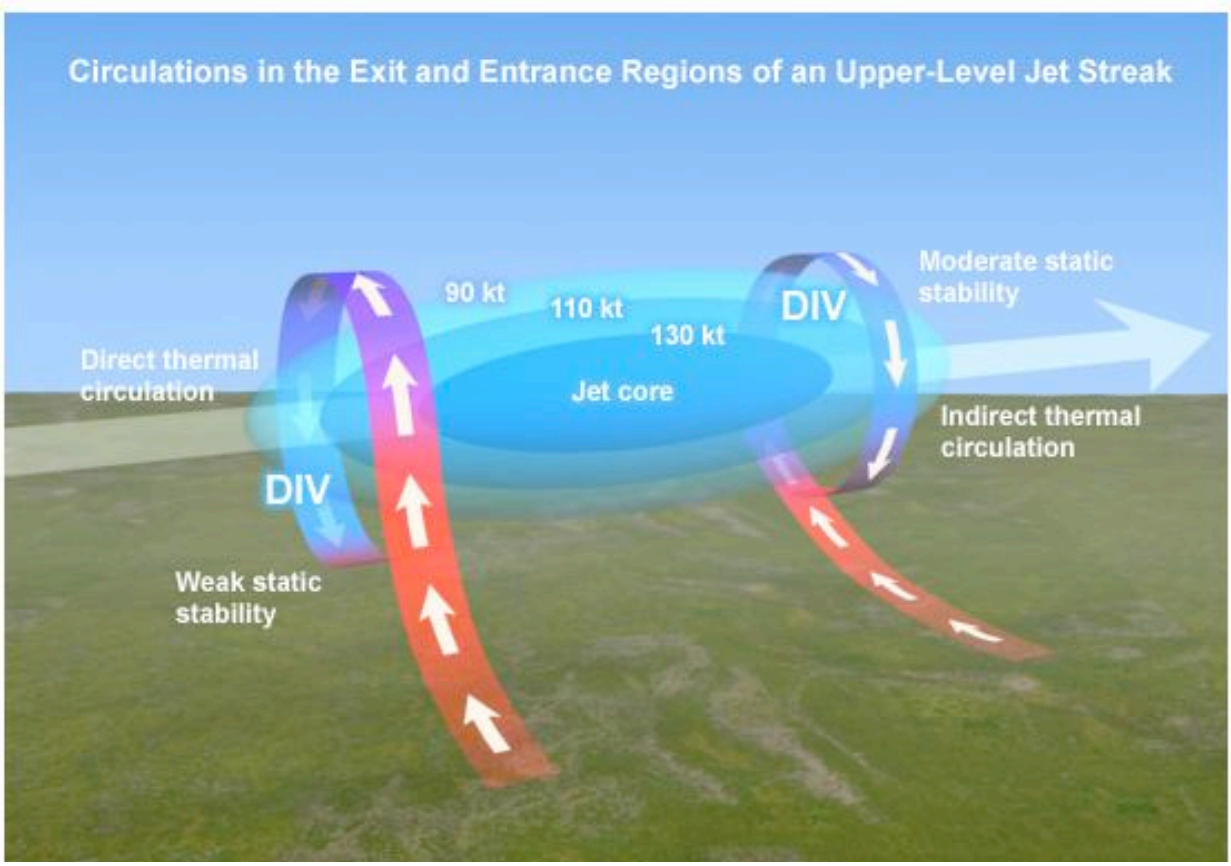

Figure 1. Conceptual model of a straight-line upper-level jet streak. The divergent right entrance (left exit) region is found to the southwest (northeast) of the jet core. Looped arrows indicate the direct (indirect) thermal circulations found in the entrance (exit) region. Image courtesy of the Cooperative Program for Operational Meteorology, Education and Training (COMET).

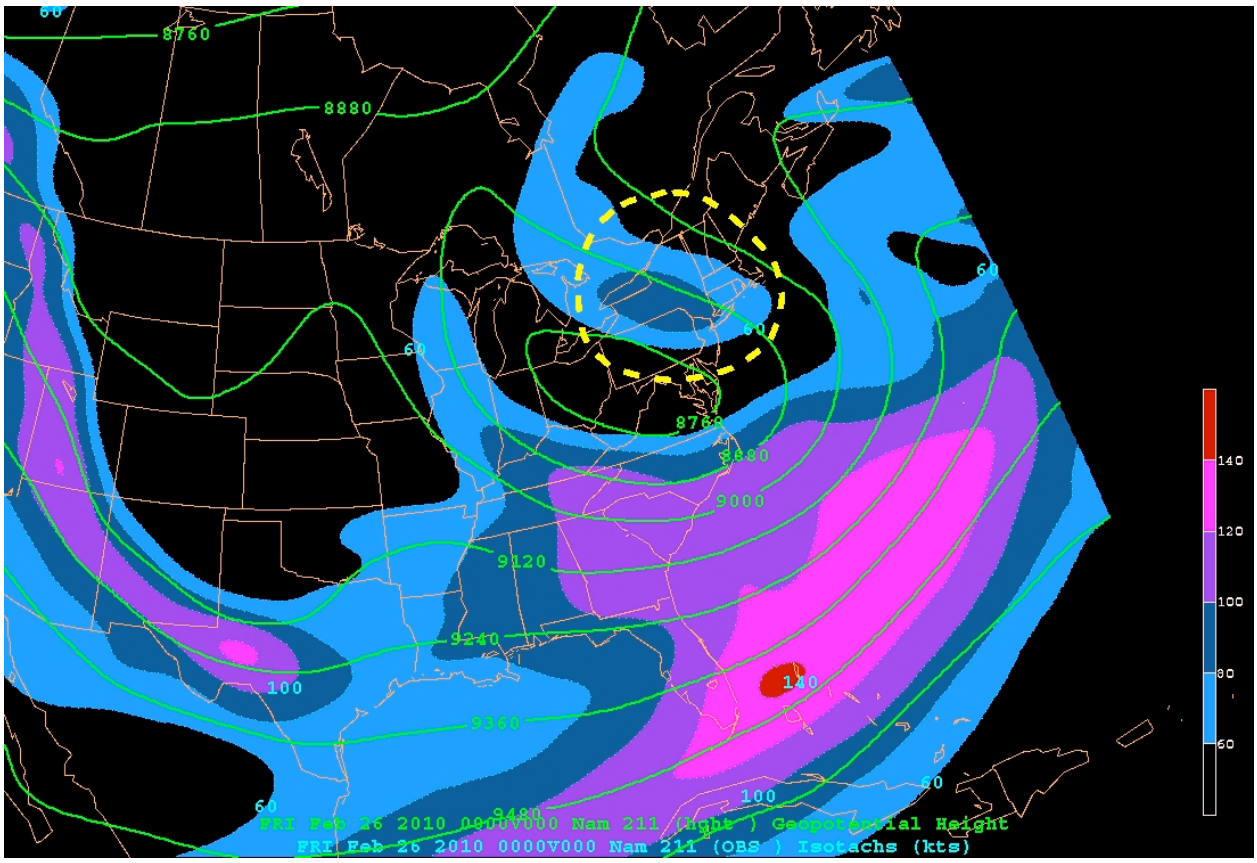

Figure 2a. North American Mesoscale (NAM) analysis of 300-hPa heights (solid green, gpm) and isotachs ≥ 60 kt (dotted blue/shading), valid at 0000 UTC 26 February 2010. Heavy dashed yellow line highlights jet streak of interest.

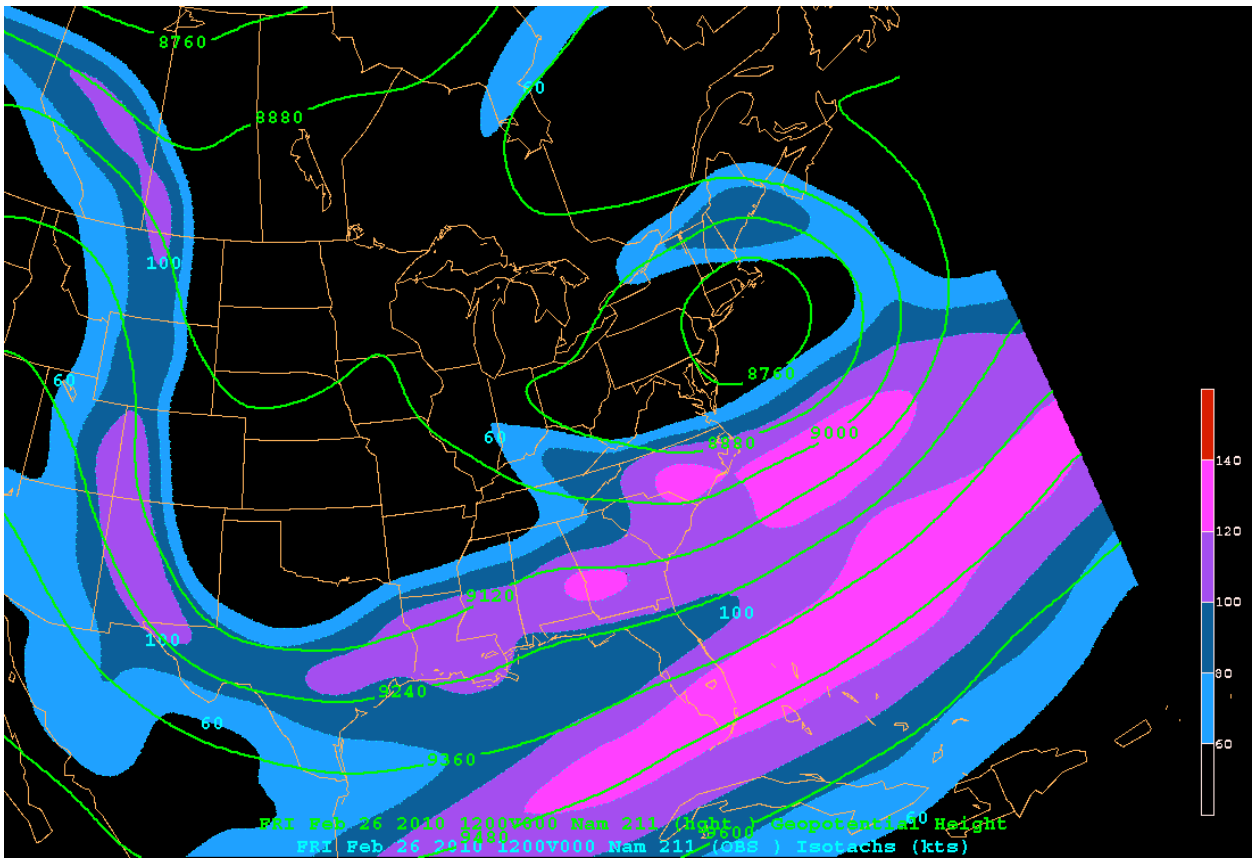

Figure 2b. North American Mesoscale (NAM) analysis of 300-hPa heights (solid green, gpm) and isotachs ≥ 60 kt (dotted blue/shading), valid at 1200 UTC 26 February 2010.

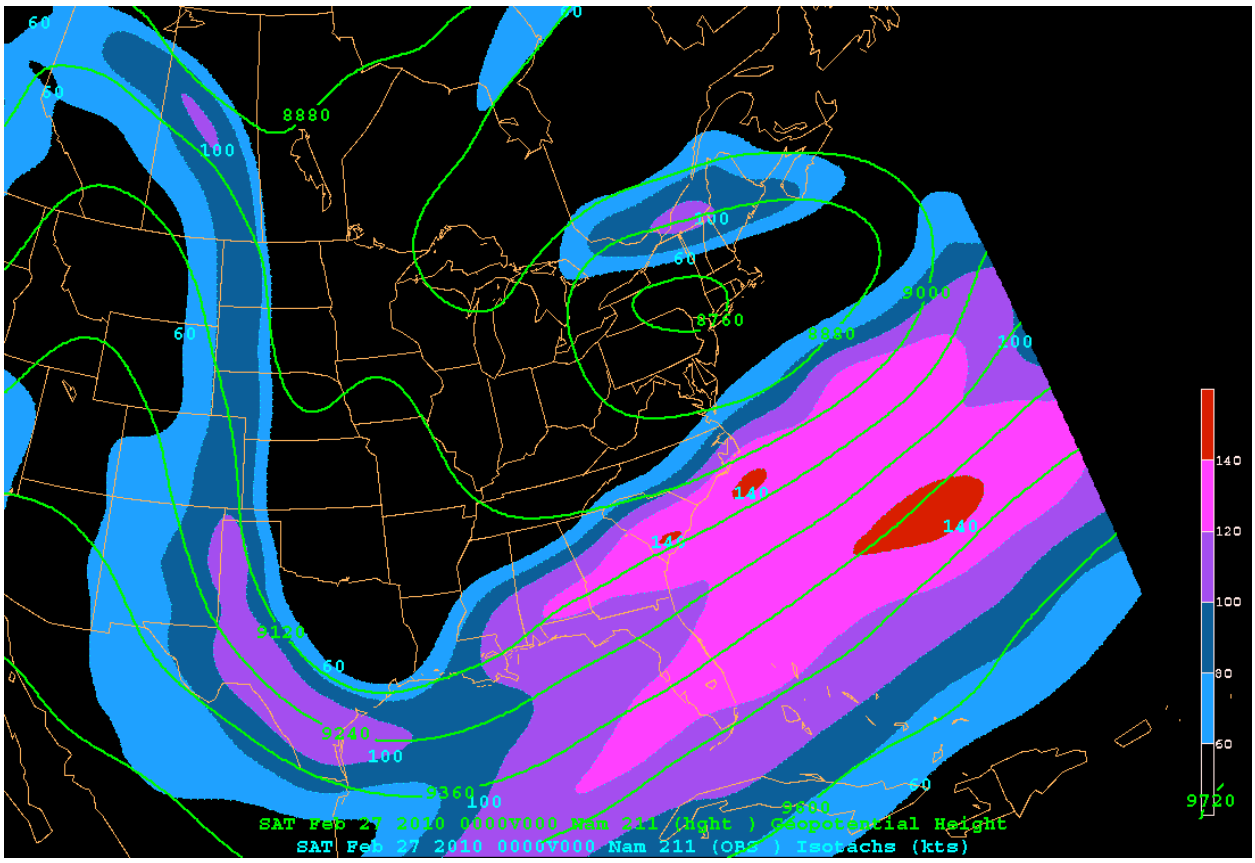

Figure 2c. As in Fig. 2b, except valid at 0000 UTC 27 February 2010.

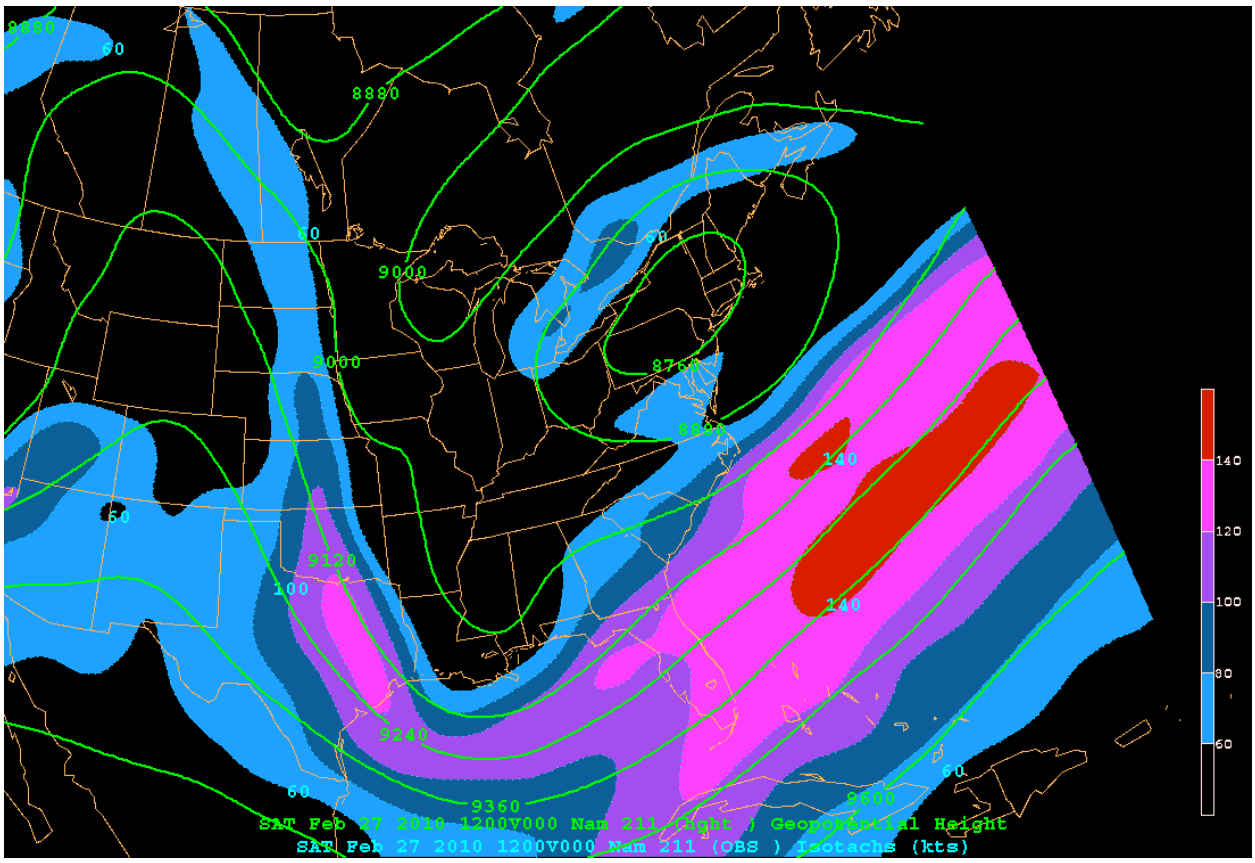

Figure 2d. As in Fig. 2b, except valid at 1200 UTC 27 February 2010.

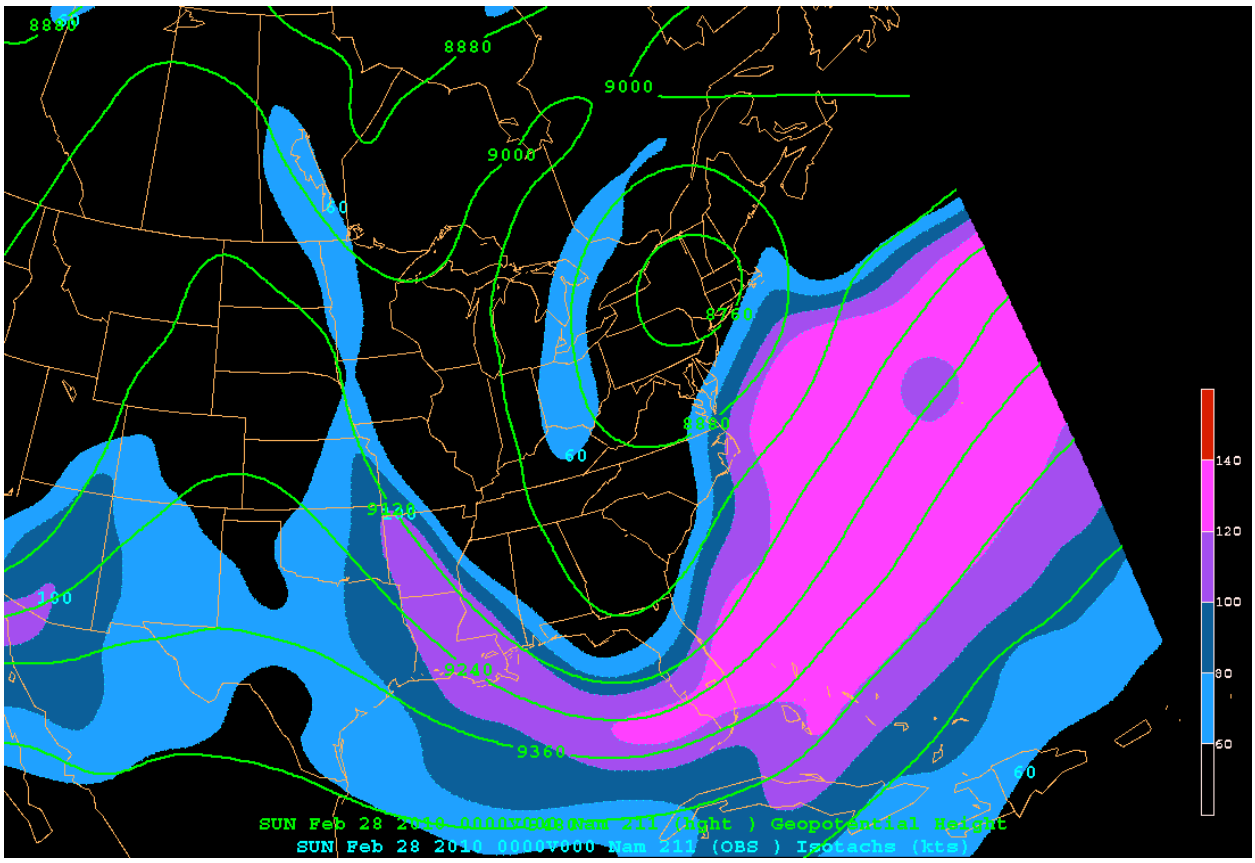

Figure 2e. As in Fig. 2b, except valid at 0000 UTC 28 February 2010.

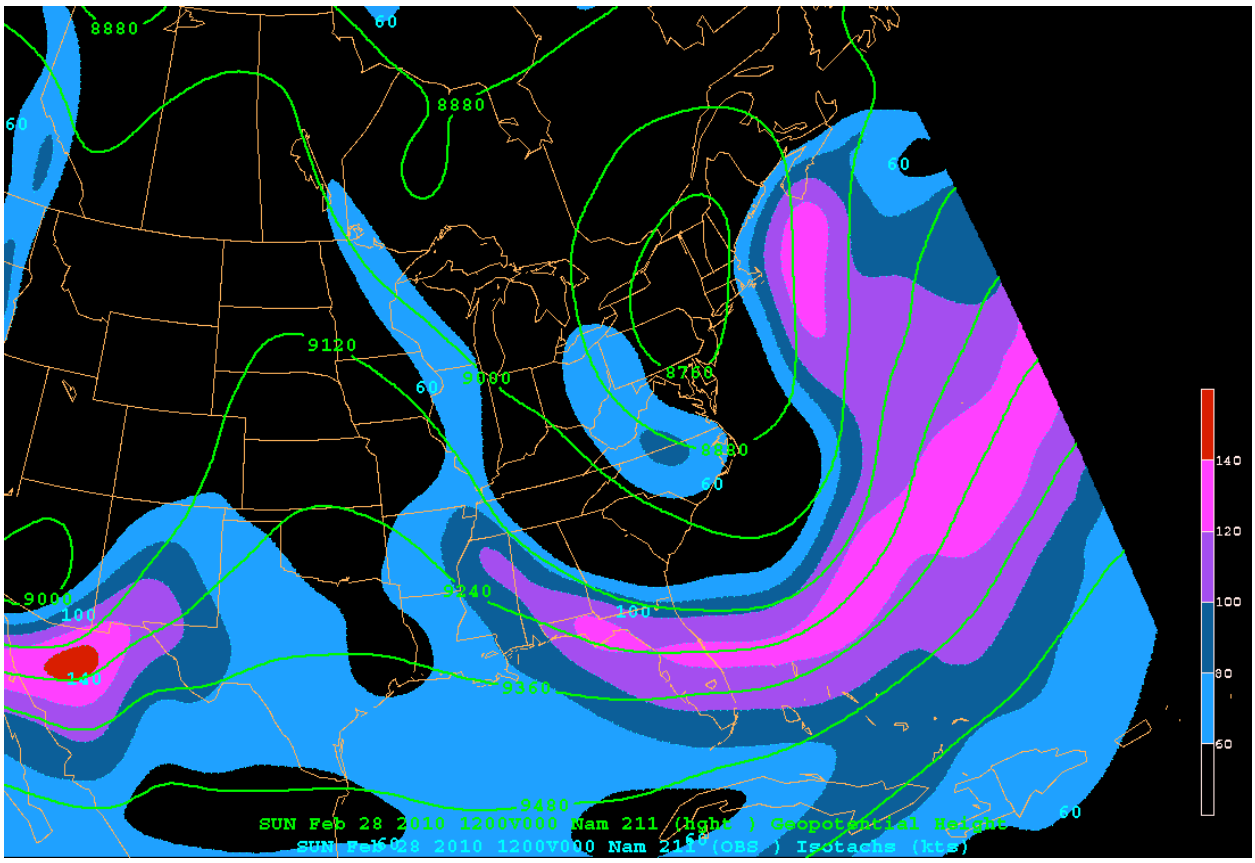

Figure 2f. As in Fig. 2b, except valid at 1200 UTC 28 February 2010.

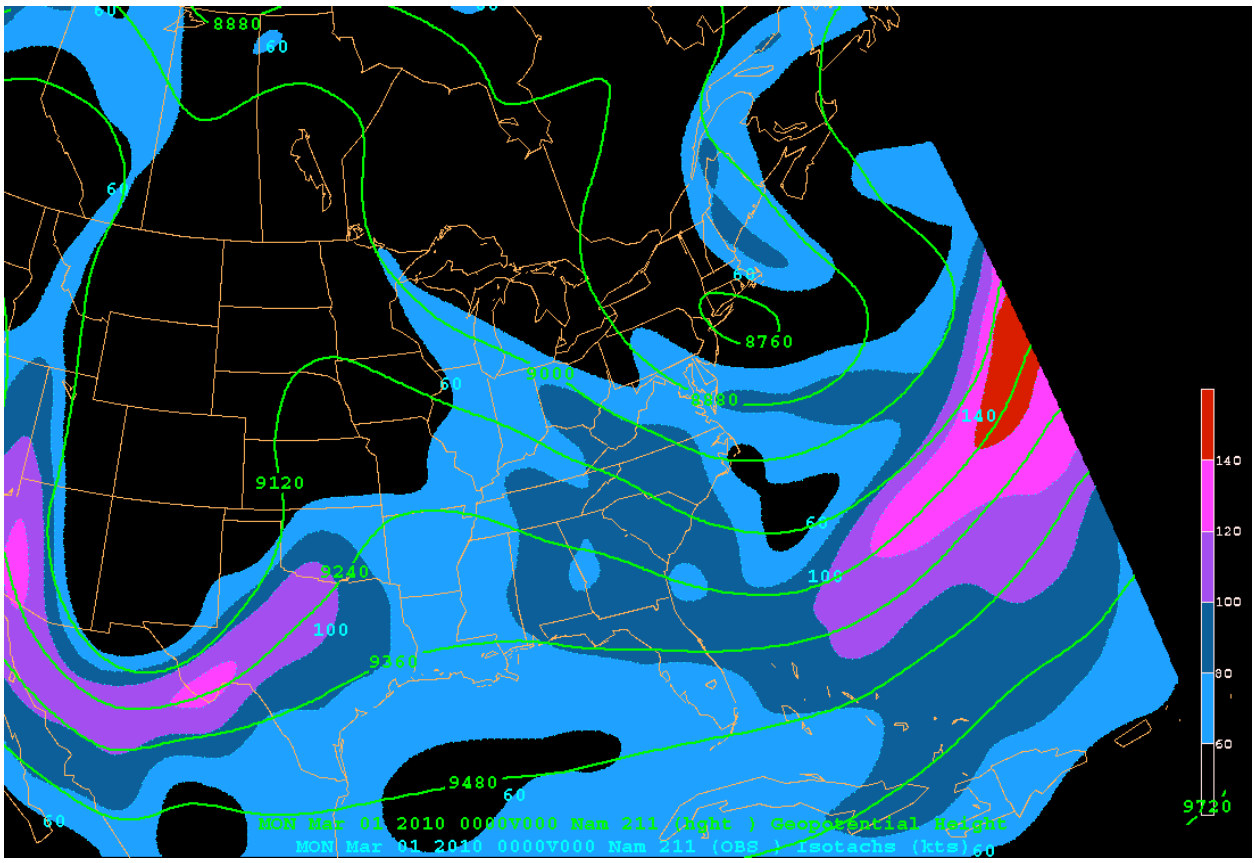

Figure 2g. As in Fig. 2b, except valid at 0000 UTC 1 March 2010.

Figure 2h. Animated loop of NAM analyses of 300-hPa heights (solid yellow, gpm) and isotachs ≥ 60 kt (shading) for the period 0000 UTC 26 February – 1200 UTC 28 February 2010. Access loop via **http://www.nwas.org/ej/2011/2011-EJ6/300hPa-Jet-Loop.gif.**

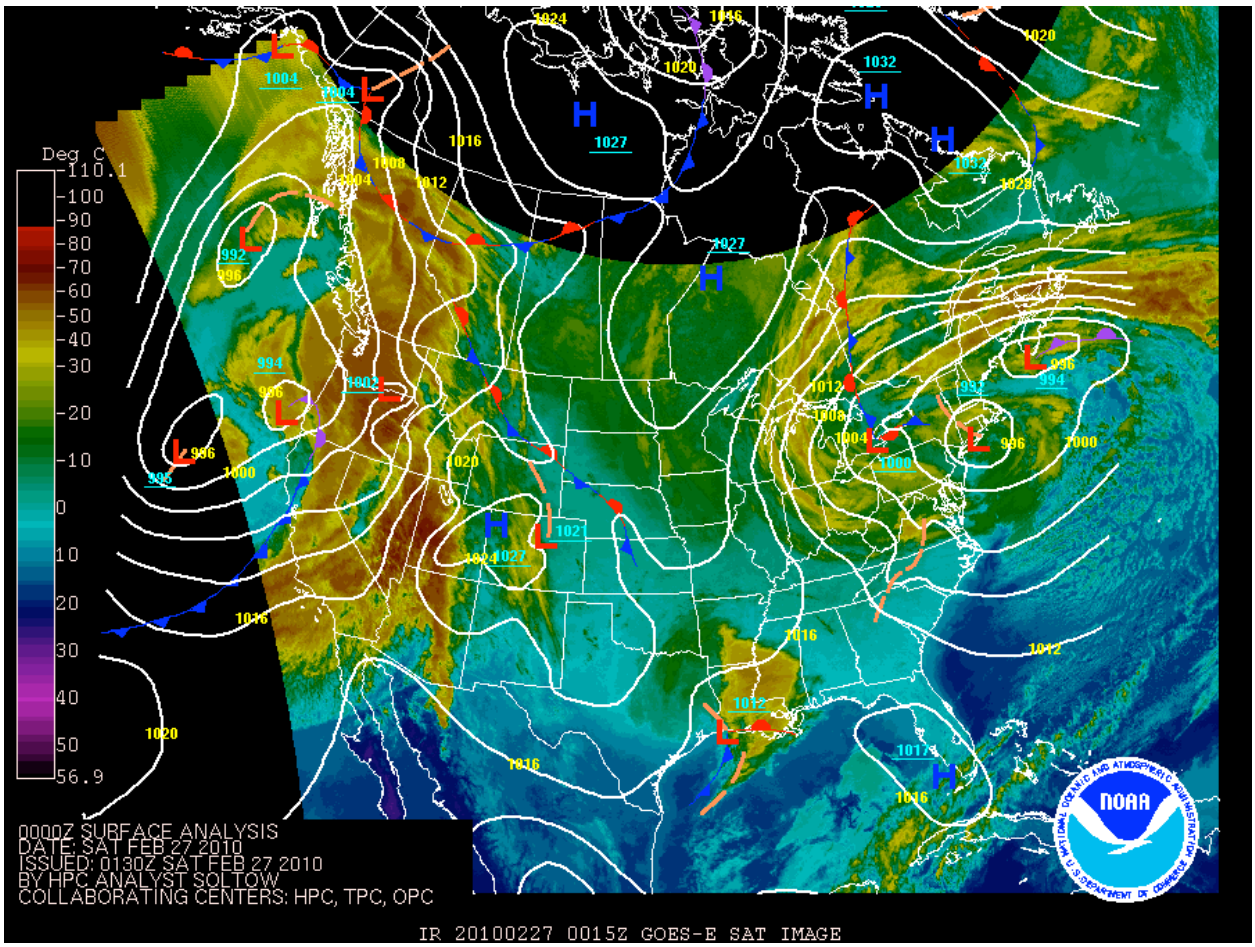

Figure 3. HPC North American surface analysis and GOES-East infrared satellite image, valid at 0000 UTC 27 February 2010. Solid white contours are mean sea-level isobars (hPa). Front and pressure system symbologies are standard.

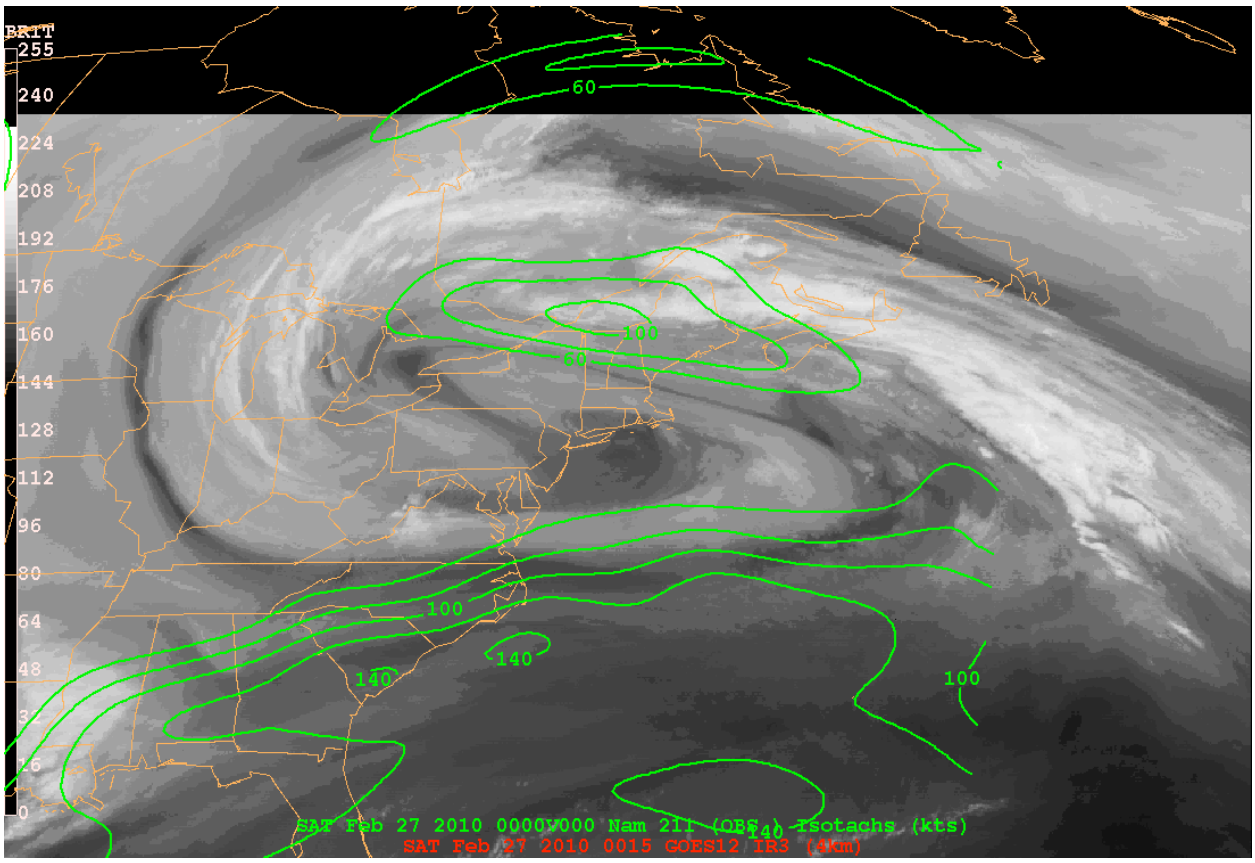

Figure 4. GOES-East water vapor satellite image and NAM analysis of 300-hPa isotachs ≥ 60 kt (green solid), valid at 0000 UTC 27 February 2010.

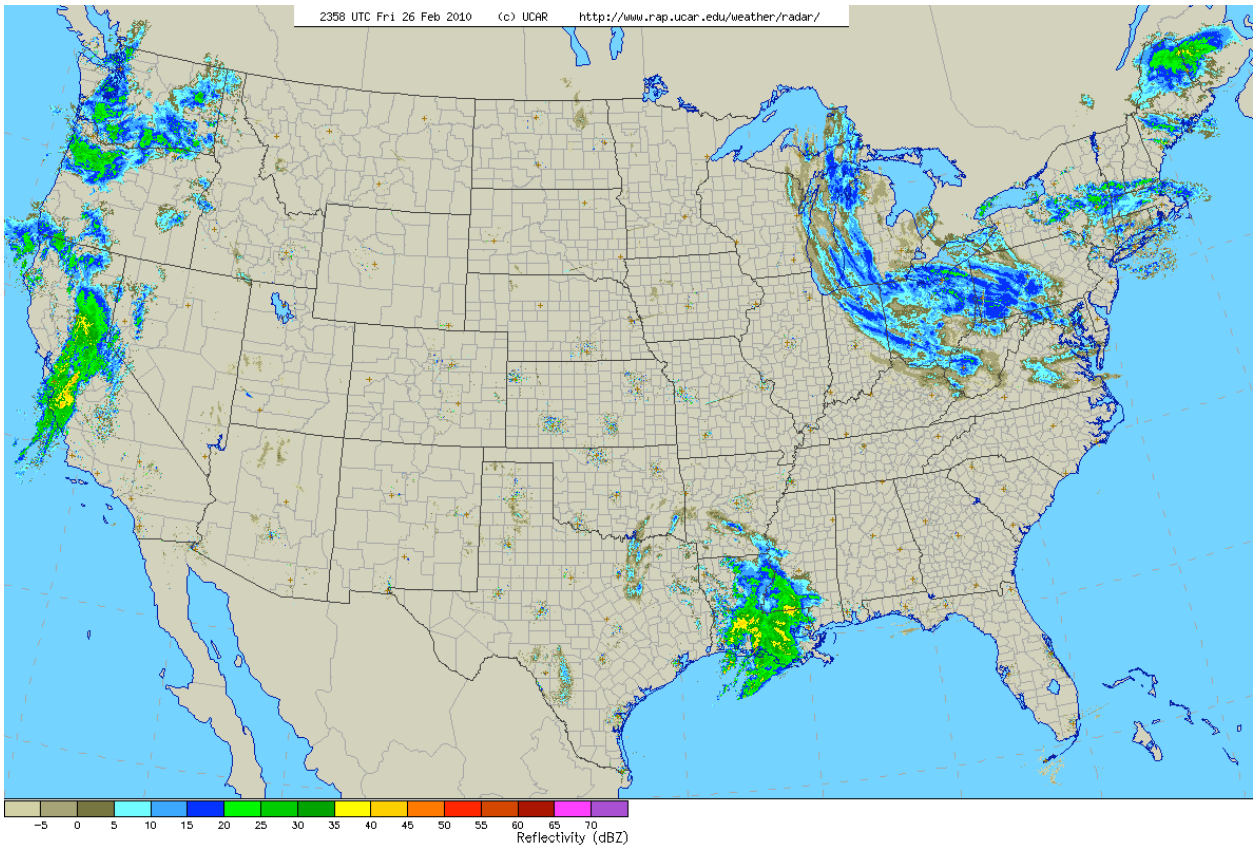

Figure 5. National 0.5˚ radar reflectivity composite image, valid at 2358 UTC 26 February 2010. Image courtesy of the University Corporation for Atmospheric Research (UCAR).

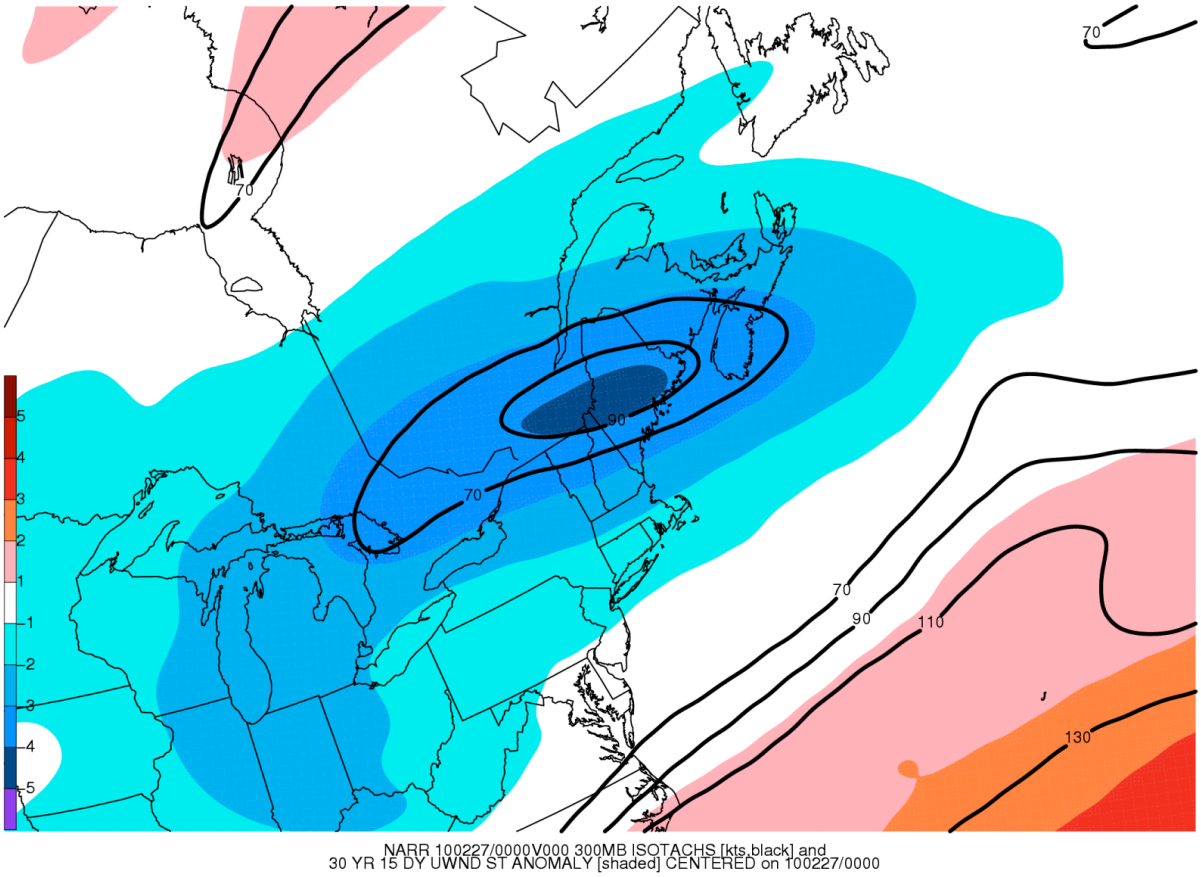

Figure 6. 300-hPa isotachs ≥ 70 kt (solid) valid at 0000 UTC 27 February 2010 and standardized anomalies of 300-hPa u-wind (shading), based on 30-year climatological values. Standardized anomalies have an interval of one standard deviation; warm (cool) colors indicate positive (negative) anomalies of at least one standard deviation.

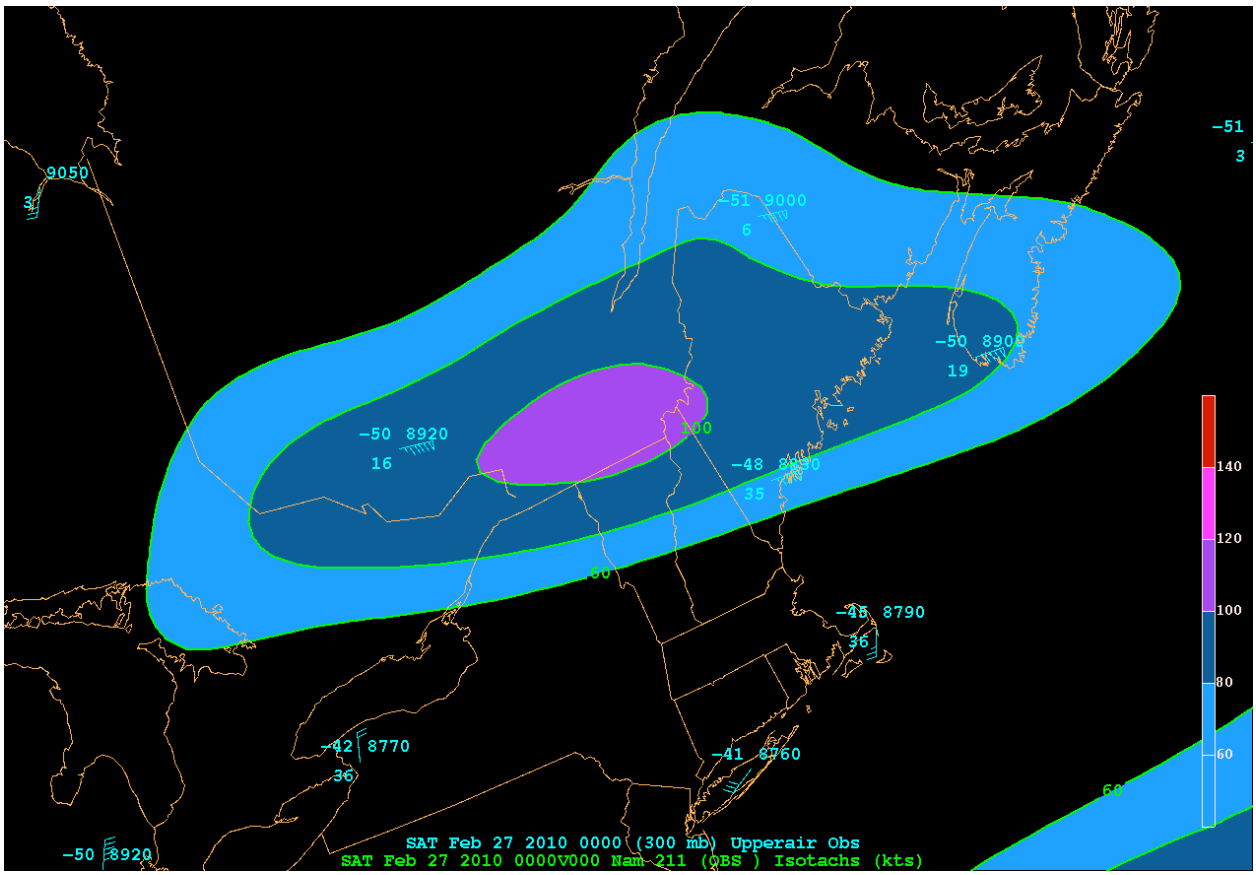

Figure 7. NAM regional analysis of 300-hPa isotachs ≥ 60 kt (green solid/shading) and rawinsonde observations, valid at 0000 UTC 27 February 2010. Observations follow standard station model format with the exception of geopotential height, which is listed in whole gpm.

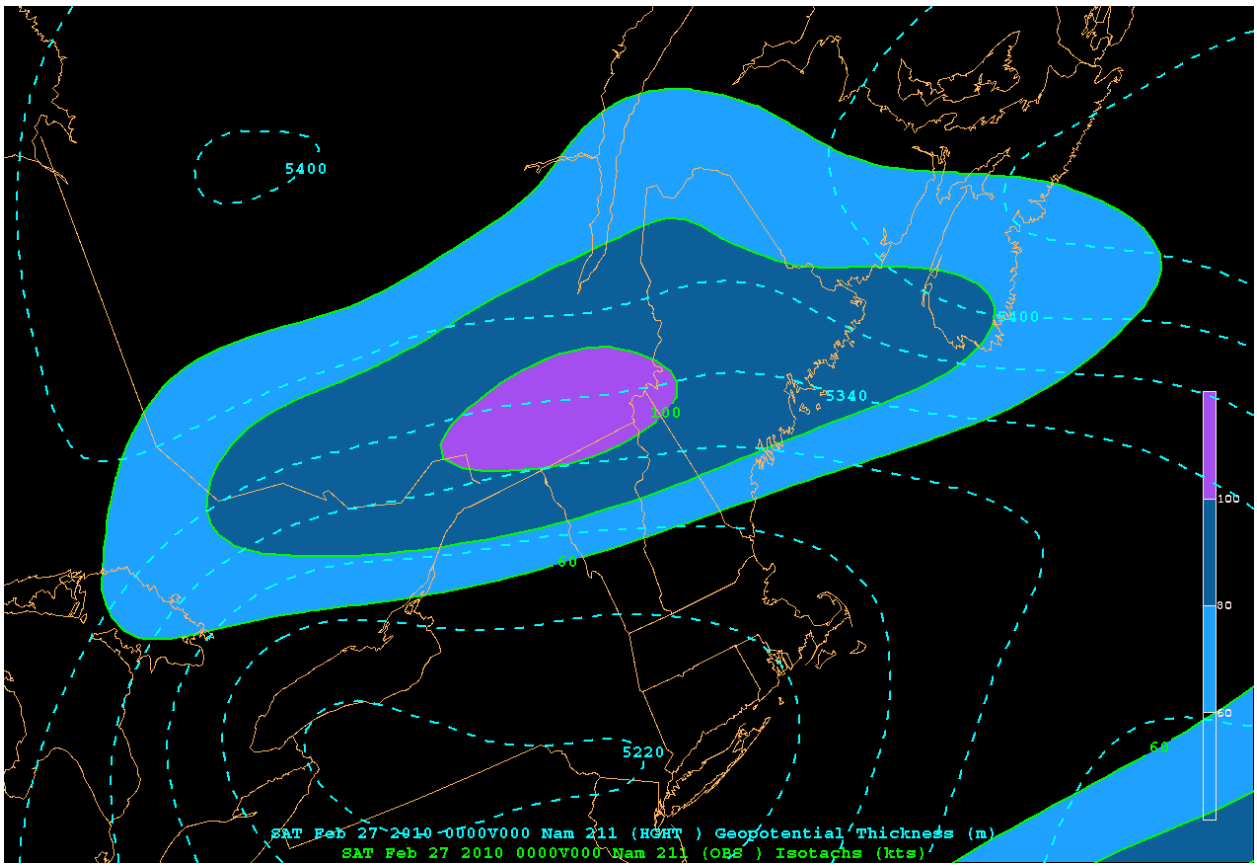

Figure 8. NAM regional analysis of 300-hPa isotachs ≥ 60 kt (green solid/shading) and 1000-500 hPa thickness (blue dashed, gpm), valid at 0000 UTC 27 February 2010.

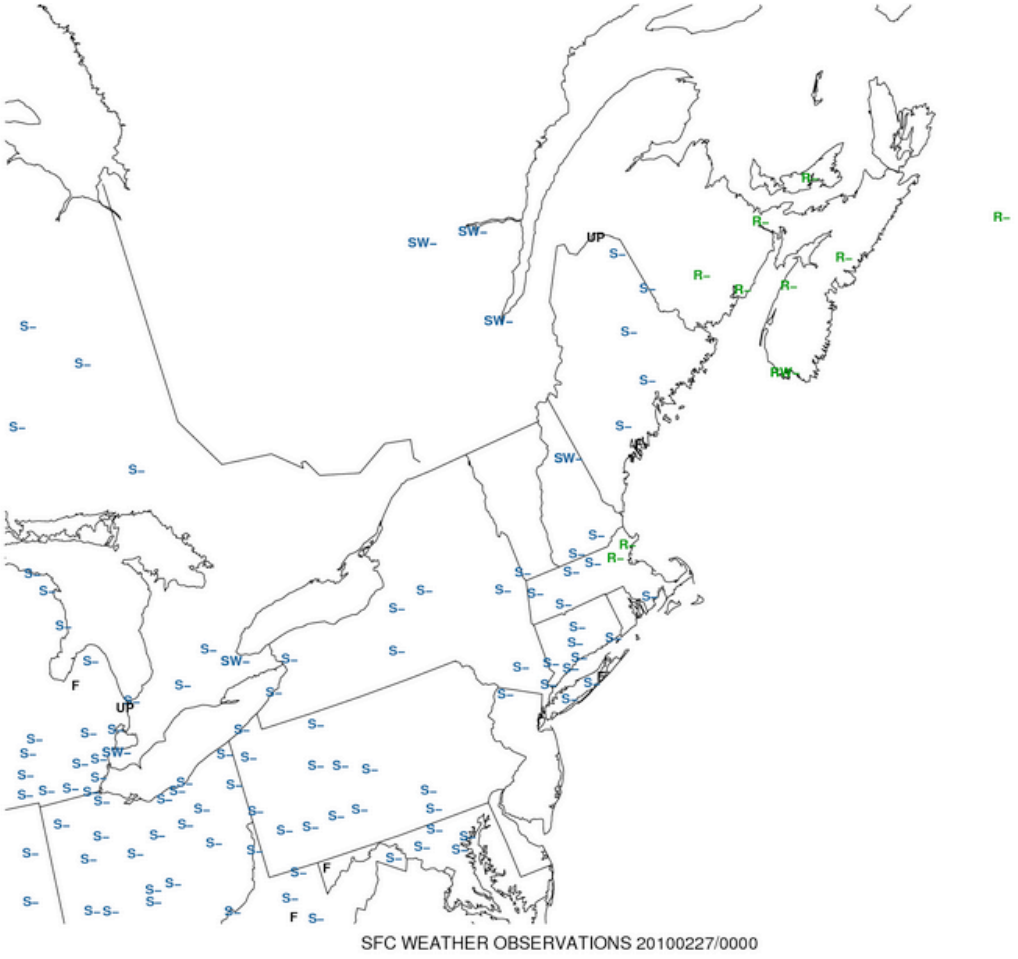

Figure 9. Surface precipitation observations valid at 0000 UTC 27 February 2010. F is fog, R- is light rain, RW- is light rain showers, S- is light snow, SW- is light snow showers, and UP is unknown precipitation.

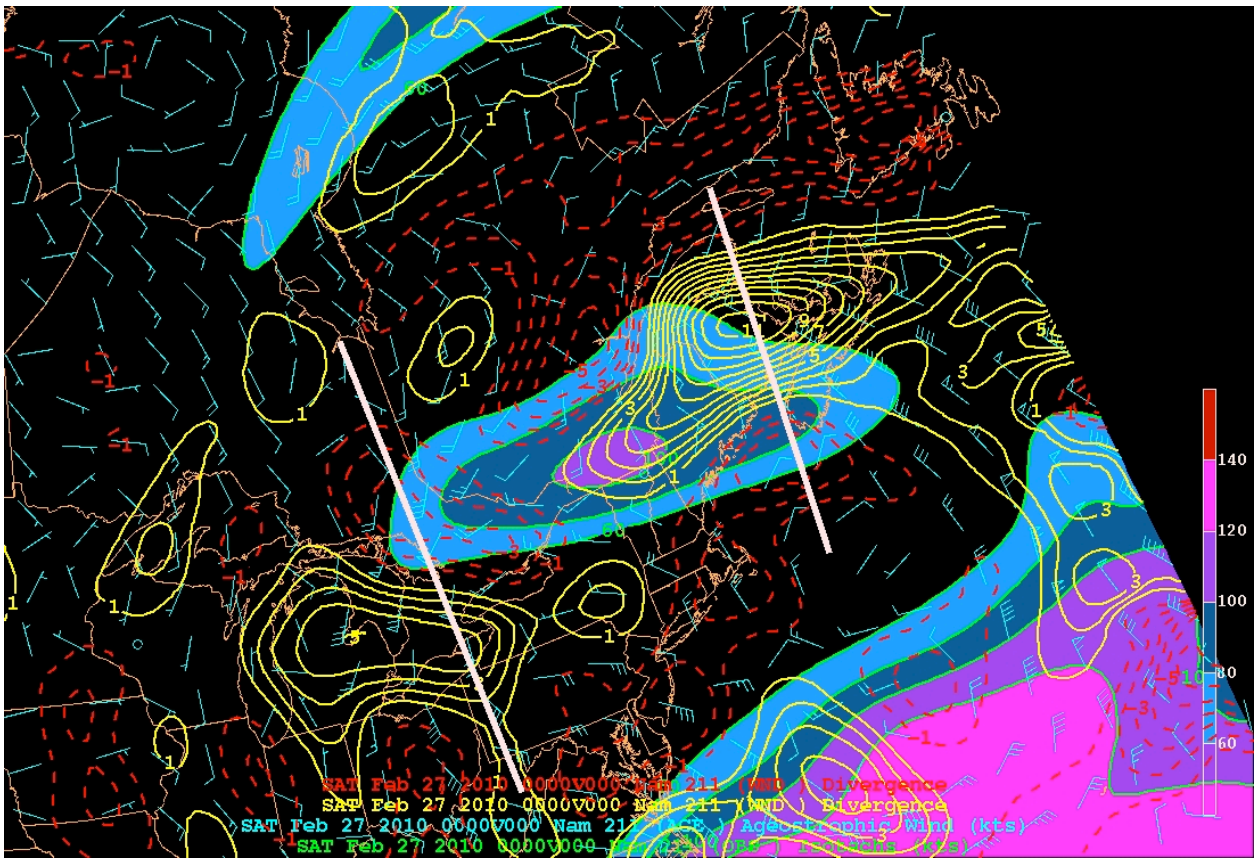

Figure 10. NAM regional analysis of 300-hPa isotachs ≥ 60 kt (green solid/shading), divergence (yellow solid, 10^{-5} s^{-1}), convergence (red dashed, 10^{-5} s^{-1}), and ageostrophic wind (blue barbs, kt), valid at 0000 UTC 27 February 2010. Cross-section axes are shown in white.

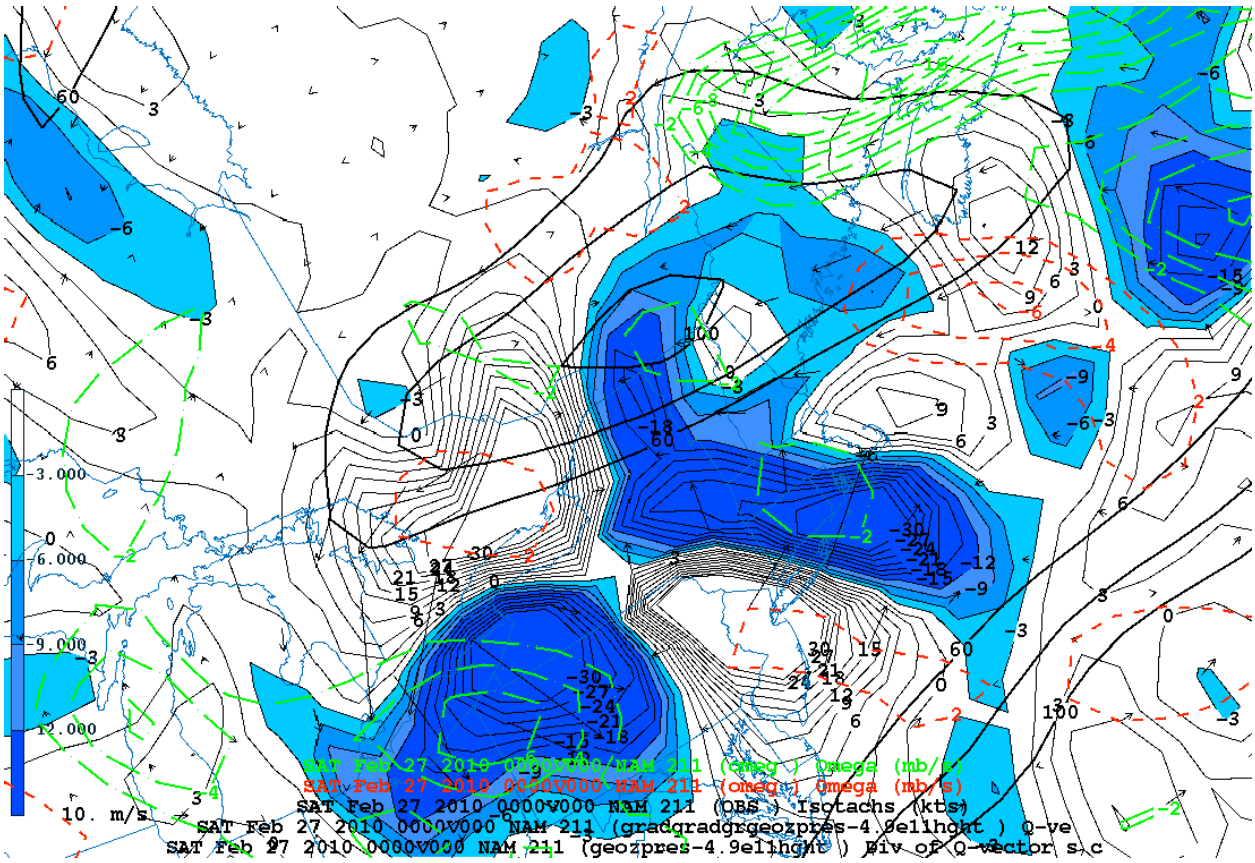

Figure 11. NAM regional analysis of 300-hPa isotachs ≥ 60 kt (thick black solid), 400-700 hPa $\mathbf{Q_s}$ (black vectors), $\nabla \cdot \mathbf{Q_s}$ (thin black, blue shading ≤ -3 x 10^{-16} K m^{-1} hPa^{-1} s^{-3}), and 500-hPa omega (green dashed negative, red dashed positive, □b s^{-1}), valid at 0000 UTC 27 February 2010.

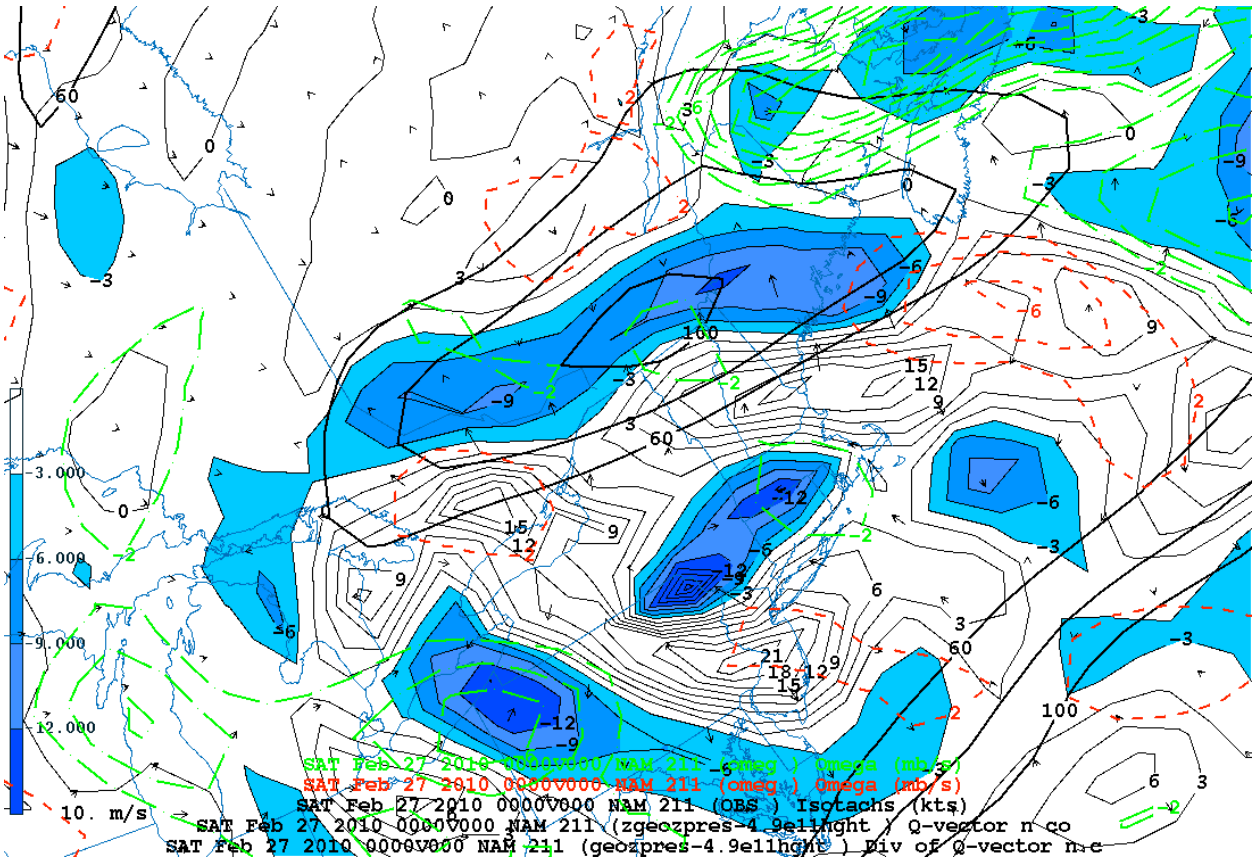

Figure 12. NAM regional analysis of 300-hPa isotachs ≥ 60 kt (thick black solid), 400-700 hPa $\mathbf{Q_n}$ (black vectors), $\nabla \cdot \mathbf{Q_n}$ (thin black, blue shading ≤ -3 x 10^{-16} K m^{-1} hPa^{-1} s^{-3}), and 500-hPa omega (green dashed negative, red dashed positive, □b s^{-1}), valid at 0000 UTC 27 February 2010.

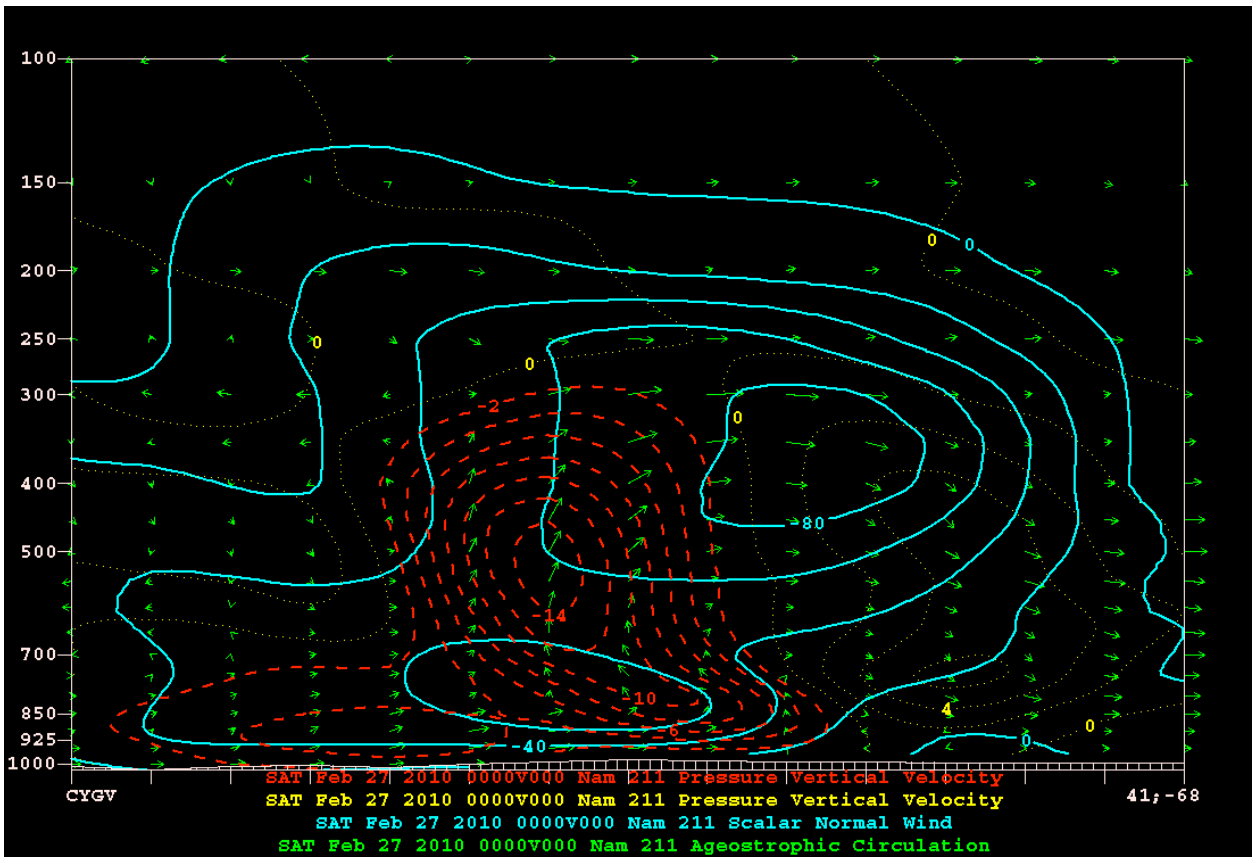

Figure 13. NAM analysis-based entrance region cross-section from Havre-Saint-Pierre, QC (CYGV, left) to 41˚N, 68˚W (right), valid at 0000 UTC 27 February 2010. Solid blue contours are plane-normal isotachs (kt). Vertical motion is illustrated as positive omega (dotted yellow, μb s^{-1}) and negative omega (dashed red, μb s^{-1}). Green arrows represent ageostrophic circulation vectors in the plane of the cross-section and model-derived vertical motion.

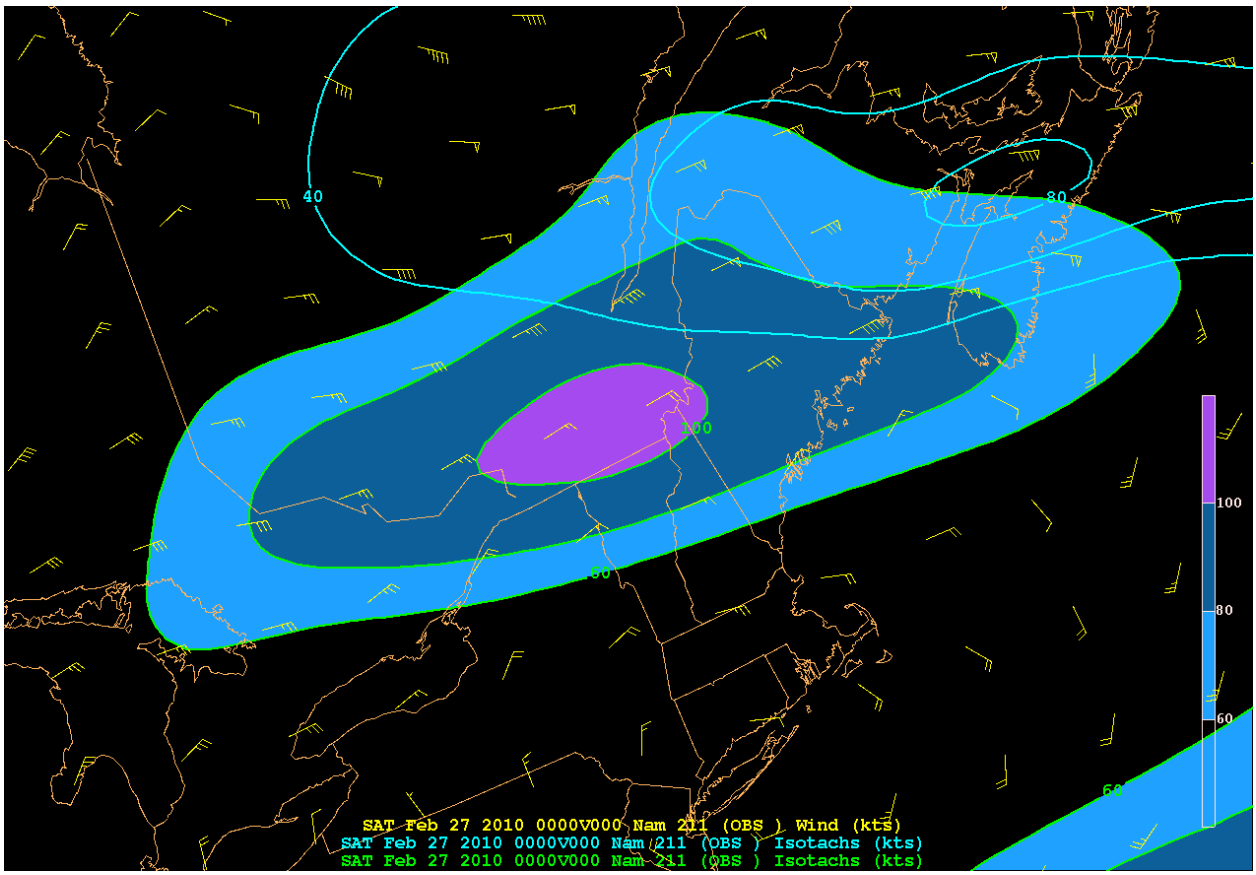

Figure 14. NAM regional analysis of 300-hPa isotachs ≥ 60 kt (green solid/shading), 850-hPa isotachs ≥ 40 kt (blue solid), and 850-hPa wind (yellow barbs, kt), valid at 0000 UTC 27 February 2010.

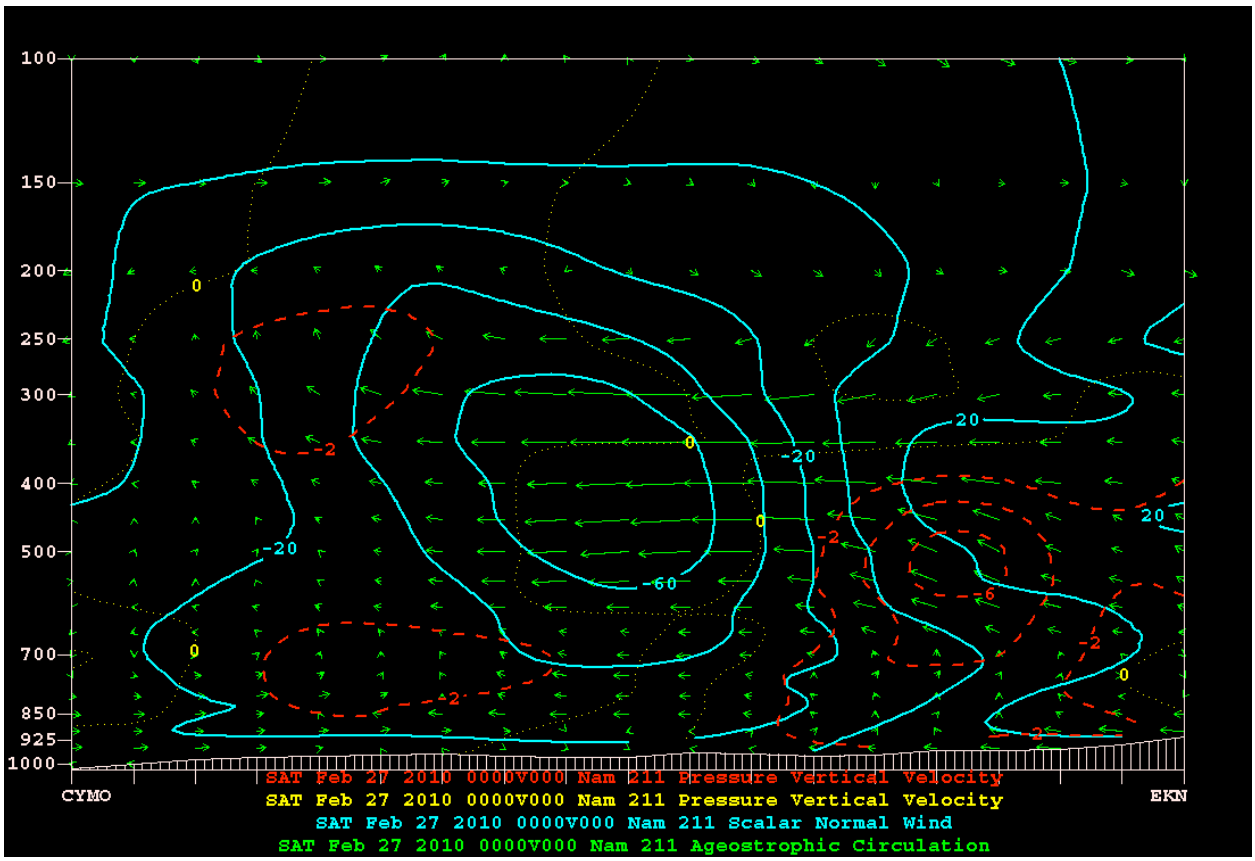

Figure 15. NAM analysis-based exit region cross-section from Moosonee, ON (CYMO, left) to Elkins, WV (EKN, right), valid at 0000 UTC 27 February 2010. Solid blue contours are plane-normal isotachs (kt). Vertical motion is illustrated as positive omega (solid yellow, μb s^{-1}) and negative omega (dashed red, μb s^{-1}). Green arrows represent ageostrophic circulation vectors in the plane of the cross-section and model-derived vertical motion.